

Implementation of Chaotic Atom Search Optimized SWIN Transformer Architecture for Efficient Corpus Callosum Segmentation in Brain MRI Images

Abstract. A crucial component of the brain that facilitates neuronal communication between the two halves of the brain is the corpus callosum (CC). Processing sensorial, motor, and sophisticated intellectual impulses is the major job of the corpus callosum, which integrates and transfers data from both cerebral hemispheres. Segmentation of the CC from brain MRIs is a highly challenging technique because of the low brightness of the surrounding organs and tissues. CNN has historically performed better in segmenting medical images, but in 2021 Microsoft researchers created a novel transformer-based structure that outperformed the prior classification methods. As a result, we propose a CC segmentation method based on the Chaotic Atom Search Optimized Swin (Shifted Window) Transformer architecture. The brain MR imaging database is collected using the open-source OASIS platform. Wavelet Thresholding preprocessing compresses the brain MR images and lowers unneeded noise. The corpus callosum is segmented from images of the skull using the proposed Swin framework, which has been developed and trained. The suggested framework is implemented in the Python environment, and metrics like accuracy, recall, precision, and F1-score are analyzed and compared with existing systems.

Streszczenie. Kluczowym elementem mózgu, który ułatwia komunikację neuronalną między dwiema połówkami mózgu, jest ciało modzelowe (CC). Przetwarzanie impulsów czuciowych, motorycznych i wyrafinowanych intelektualnych do głównego zadania ciała modzelowego, które integruje i przesyła dane z obu półkul mózgowych. Segmentacja CC na podstawie rezonansu magnetycznego mózgu jest techniką bardzo wymagającą ze względu na niską jasność otaczających narządów i tkanek. W przeszłości CNN radziło sobie lepiej w segmentacji obrazów medycznych, ale w 2021 r. badacze firmy Microsoft stworzyli nowatorską strukturę opartą na transformatorach, która przewyższała wcześniejsze metody klasyfikacji. W rezultacie proponujemy metodę segmentacji CC opartą na architekturze transformatora Chaotic Atom Search Optimized Swin (Shifted Window). Baza danych obrazowania MR mózgu jest gromadzona przy użyciu platformy OASIS typu open source. Wstępne przetwarzanie Wavelet Thresholding kompresuje obrazy MR mózgu i obniża niepotrzebne szумy. Ciało modzelowe jest segmentowane na podstawie obrazów czaszki przy użyciu proponowanego modelu Swin, który został opracowany i przeszkolony. Sugerowany framework jest zaimplementowany w środowisku Python, a wskaźniki takie jak dokładność, przypominanie, precyzyja i wynik F1 są analizowane i porównywane z istniejącymi systemami. (Implementacja zoptymalizowanej architektury transformatora SWIN w zakresie wyszukiwania atomów chaotycznych w celu zapewnienia efektywnej segmentacji ciała modzelowego w obrazach MRI mózgu)

Keywords: Corpus Callosum (CC), Wavelet Thresholding, MRI, chaotic atom search optimized (CASO) and Swin (Shifted Window) Transformer.
Słowa kluczowe: Ciało modzelowe (CC), próg falkowy, MRI, zoptymalizowane wyszukiwanie atomów chaotycznych (CASO)

Introduction

The Corpus callosum (CC) shown in Figure 1 is the largest structure made up of white matter in the central nervous system [9]. It is responsible for connecting both sides of the brain and facilitating the two. The significance of CC extends well beyond the brain's ability to form connections with other regions. Variations in its form and size have been associated with specific topic features, like sex, age, and handedness, and, more importantly, with several diseases [16]. A correlation between CC loudness and neurodegenerative or inflamed conditions, such as Alzheimer's disease and multiple sclerosis, has been reported in various studies [14]. Many disorders of the central nervous system, like dyslexia, epilepsy, and schizophrenia, along with other common clinical disorders including tobacco use, alcohol abuse, and fat appear to affect the CC. These particular kinds of conditions have the potential to transform the corpus callosum structure by modifying its form as well as volume. Clinical and scientific studies that rely on imaging data typically begin with CC segmentation to confirm and follow changes in form and volume, as well as extract morphological and physiological parameters on the CC [6].

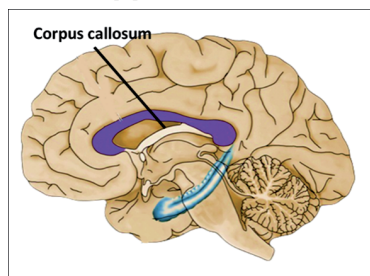


Fig. 1. An electromagnetic flow meter: principle of operation (left) and sample shape of the coil (right)

By breaking the CC into smaller pieces, we may do

cross-sectional studies, in-depth analyses of certain groups, and in-depth characterizations of specific individuals. However, CC segmentation via MRI is difficult due to shape variability across subjects, the CC's similarity to neighboring structures like the fornix, intensity variability across scanners, the partial volume effect caused by a limited acquisition resolution, and artifacts caused by technology constraints, such as motion [12]. An MRI scan of the brain can detect abnormalities such as tumors, infections, inflammation, injury, stroke, or vascular issues, as well as diseases such as bleeding, swelling, or abnormal brain development [17]. The MRI can also aid in the investigation of headaches and epileptic fits. There is a subset of the Vision Transformer known as the Swin Transformer. Computation complexity is linear in input image size since self-attention is only evaluated within each local window, and hierarchical feature maps are constructed by combining picture patches (shown in grey) in deeper layers (shown in red). CASO is a stochastic method for solving optimization problems that rely on the collective intelligence of a population. Many optimization issues are solved with CASO, which is a population-based metaheuristic optimization algorithm. This research introduces a Chaotic Atom Search Optimized Swin (Shifted Window) Transformer architecture method for Efficient Corpus callosum segmentation Brain MRI Images.

Literature Survey

CC can act as a notable biomarker for many neurological disorders such as alzimers, parkinsons, cognitive impairment and autoimmune disorders, for instance childhood-onset systemic lupus erythematosus (cSLE) [15, 2]. The article [7] provides a comprehensive assessment of previous research on computational approaches, with a particular emphasis on Corpus Callosum segmentation and percolation based on magnetic resonance imaging data. The research [10] shows

that there is a lag time between the kinetics of an impact and the strain experienced by the brain's deepest structure, the corpus callosum. A hybrid Whale and Gray-wolf optimization technique is proposed in [11] which achieved an accuracy of 90% in classification of normal brain images from abnormal images and 92% accuracy in segmenting CC. Research [8], proposed a deep-learning strategy for Corpus Callosum segmentation. The therapeutic analysis may make use of feature extraction and classification arrangement based on segmentation results in the future. In the study [3] the splenium of the CC is the last section of the structure. Embryonic development, architecture, vascularization, function, imaging of disease, potential pathophysiological pathways leading to pathology, and clinical implications are all covered. The study [4] adds to the growing body of data showing age-related regionally selective abnormalities in white matter architecture and shows that high gradient dispersion MRI might be sensitive to the axon white matter substrate in the elderly degradation shown in conventional Diffusion tensor imaging (DTI) measures. The purpose of the research [13] is to identify the mechanisms by which the skull moves and causes brain deformation that reaches deep brain areas. Specifically, they looked at how head movement, falx displacement, and corpus callosum injury are all connected. Two separate groups of kids were used in this research. Diffusion tensor imaging, neurite orientation dispersion and density imaging, and apparent fiber density metrics are all the results of analyzing data from multi-shell diffusion MRI scans. Each diffusion metric was analyzed in a multivariate profile format over all 10 sub-regions of the Corpus callosum [5]. The research [18] investigates the relationship between the disability level of multiple sclerosis patients and the CC index and brain volumetric. The Corpus callosum(CC), the volume of cortical grey matter, the volume of subcortical grey matter, and the volume of white matter make up the volumetric of the brain. The study [1] was to determine whether or not the g-ratio MRI measurement can be utilized to accurately predict conducting lags in CC. To describe the conducting delays of long-range white matter fibers, we propose a complete structure for doing so. Within this framework, the structural features of fibers are included in a model of axon conduction based on biophysics.

Problem Statement

The corpus callosum has been the focus of several studies on the topic of MRI segmentation. In more recent research, many supervised segmentation techniques utilizing deep learning have been developed. Because of this, the training phase of deep learning requires a substantial amount of data. Because the DICOM (DCM) data they have collected are restricted and come in a variety of formats, employing a deep learning technique would need a great deal of time and some preprocessing steps. Unsupervised learning, which may be utilized in methods like clustering and contour evolution and does not require Heavy amounts of information for the training process, is still another way that can be employed. This method can be used instead of supervised learning. Unsupervised learning, on the other hand, offers a quick approach to segmentation in image processing. Unsupervised learning has many drawbacks, one of which is a level of accuracy that is significantly lower than that of supervision of learners. In this study, we recommended Chaotic Atom Search Optimized Swin (Shifted Window) Transformer architecture for efficient CC segmentation in Brain MRI images.

Proposed methodology

The simplicity of use and adaptability of the algorithms that make up swarm intelligence has piqued the interest of academics who are looking for solutions to challenges that are specific to their fields. Ant Colony Optimization (ACO), Particle Swarm Optimization (PSO), Artificial Bee Colony Optimization (ABC), and a number of other algorithms are examples of well-known optimization methods. The CASO algorithm is one of these, and it was modeled after the behavior of fish schooling or flocking of birds. Whatever this algorithm does is find the best solution to a problem in an iterative manner by utilizing the local best and the global best that was obtained from the previous iterations. Among these algorithms, the CASO algorithm is considered to be the most effective. In this study, we proposed the implementation of Chaotic Atom Search optimized Swin (shifted window) transformer Architecture method for Efficient Corpus callosum segmentation Brain MRI Images. A diagram of the proposed method is presented in Figure 2.

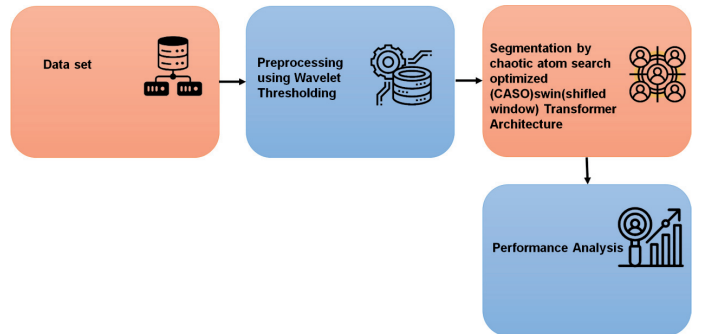


Fig. 2. Block Diagram of Proposed Method.

OASIS Brains Dataset

This set is a cross-sectional collection that includes 416 participants ranging in age from 18 to 96 years old. There are three or four separate T1-weighted MRI images acquired for each person during a single scanning session. These scans are included. All of the individuals are right-handed, and they are a mixed group of males and females. One hundred of the patients over the age of 60 who were above in the research were given a clinical diagnosis ranging from extremely mild to severe Alzheimer's disease (AD) [19]. In addition, a reliability data set that includes 20 healthy participants who had imaging on a later visit during the first three months after their first session is also included in the package.

Wavelet Thresholding

Wavelet Threshold denoising is an analytical technique that employs time-frequency to choose the optimal frequency range by the properties of the images. Over time, an image specifies different physical qualities. An image that is undesirable and interferes with the BM images conveying the actual image is called noise. This algorithm is a more simple and computational technique. By using a chosen BM image wavelet basis, an orthometric $M \times M$ matrix Z is approximately built in which it forms to the discrete wavelet transform (DWT).

$$(1) \quad a = Zy$$

Where $y = [y(1), y(2), \dots, (in)]$, $a = [a(1), a(2), \dots, a(M)]$ includes the wavelet coefficients that were produced. Any wavelet coefficient c_i follows a normal distribution with variance and mean equal to the

corresponding coefficient value of BM image of the noiseless bone marrow image y since matrix Z is orthogonal(h). The BM image is anticipated to distribute the complete energy of $y(h)$ in only a few wavelet components, which lends itself to large amplitudes, assuming that the image under consideration is sparse in the wavelet domain, which is typically the case. As a result, the noise alone is responsible for the amplitude of the majority of wavelet components. The basic idea of wavelet thresholding is to subtract from one another all the components that fall below a noise threshold, $S = \sigma A$, where A is a constant, and then to rebuild the denoised image $y(h)$ using only the higher amplitude components. The thresholding operators are defined as below:

$$(2) \quad \rho_S(y) = \begin{cases} x, & x > S \\ 0, & x \leq S \end{cases}$$

By using the above thresholding operators the predicted de-noised bone marrow image is given by

$$(3) \quad y = Z^S a$$

Where, $S\rho_s(a_1), \rho_S(a_2), \dots, \rho_S(a_M)$, and Z^S denotes the transposition matrix bone marrow image of Z .

Segmentation using chaotic atom search optimized and Swin (Shifted Window) Transformer

The segmentation method may now take in the cleaned and prepared data set. Chaotic Atom- Search Optimization Swin transformer architecture is employed to do the data set segmentation in this study.

The Chaotic are able to move because of their ability to 'glide'. Acorn nuts make up the majority of their diet, thus they must often change positions in order to get enough to sustain themselves. Animals make it very challenging to meet their needs, especially during the colder months when leaf drop is common. During the colder months, the Chaotic is less active. They keep looking for excellent foods that can be stored for the off-season, such beech nuts. After hibernating during the winter, the Chaotic reawaken their appetites and return to the world in search of sustenance. Compared to more orderly randomness, the kinematic and probabilistic features of chaos are more extreme. Modifying even a few of its traits or initial conditions might have a profound effect on how it develops and evolves. Accordingly, we combined the concepts of Chaotic and chaos to create the Chaotic Atom Search Optimization (CASO). It is generally accepted as extremely successful in intelligence optimization algorithms, and this is because it guarantees a diversity of created solutions.

The values for all of the constants, including the population size, the maximum number of iterations that will be performed, and the lowest and maximum boundaries, are being set to their initial values. The positions of each jumping squirrel throughout dimensional space are assigned according to the unpredictability of chaos.

The fitness function acts as a guide for the optimization process, with the objective role playing the part of the one being optimised. Depending on the method of elimination, the intended functionality may require revision. The fitness function's outputs are then utilised to pinpoint the origin of the EEG reading. After the locations of the EEG signals are sorted in ascending order, they may be categorised.

The leaping Chaotic exploratory behaviour is altered because of the existence of managed predators. EEG signals

are more likely to be distorted if they are in the centre of the frequency range and hence further from their ideal signal. Since these are the only artefacts from the time period in question, we may expect that any potential for bias will be reduced.

To avoid predators, leaping Chaotic on an oak tree typically go to a nearby beech tree. Therefore, the new position may be formed by employing probabilities of emergence and random placement.

Jumping Investigations Depending on the season, people may act more or less erratically. To do this, we develop an EEG signal removal constant and perform a minimum removal computation to determine whether or not the artefact will be eradicated.

After satisfying the optimization criterion, the EEG signal will migrate to a site chosen at random, as the responses can come from any direction and might be located anywhere on the scalp. This might be explained with the help of a virtual model, and a virtual model creator is used to make a more recent version of this.

Although the more recent stance has been established, it is still feasible that the older one was superior. So after each set, we have to compare the current value of the EEG signal's fitness to its prior value to see whether there has been any improvement. If an older fitness value is chosen over a newer one, the position of the EEG signal will not shift.

Hierarchical vision transformers called Swin transformers have been presented as a means of computing self-attention using a shifted window partitioning approach. Consequently, Swin transformers apply to a wide range of downstream applications, where the extracted multi-scale characteristics may be put to good use.

Except at Stage-3, when there are six simultaneous Swin Transformer (ST) Blocks, the Swin Architecture always consists of at least two consecutive ST Blocks. Figure 3 shows the ST Block. ST is constructed by swapping out the Multi-head self-attention (MSA) module typically found in a transformer block for a shifted-windows-based MSA module while maintaining the integrity of the remaining layers. An example of an ST block is depicted in above figure; a shifted window MSA module and a GELU nonlinear 2-layer MLP are its constituent parts. Each MSA unit and MLP should begin with a Layer Norm layer is utilized, and after each module, a residual connection is applied. All right, so everything saves the concept of moved windows-based attention is the same as in ViT. Therefore, it is the next step to do before exploring the Swin Transformer Block's actual implementation in code.

Both the original Transformer design and the modified version used for Corpus callosum classification use global self-attention, which calculates the connections between each token in a dataset. Many vision issues necessitating a massive quantity of tokens for detailed forecasting or to depict a good-resolution image are inappropriate due to the worldwide computing exponential complexity with regard to the number of tokens. We suggest computing self-attention inside local windows in order to maximize modeling efficiency. Each window is sized and positioned such that it does not overlap any other windows in the image. The self-attention module based on windows cannot make connections between windows, which severely restricts the scope of the models it may produce. We present a Shifted window partitioning strategy, which switches between two partitioning configurations in successive ST blocks to create Cross window connections whereas keeping the fast calculation of no-overlapping windows.

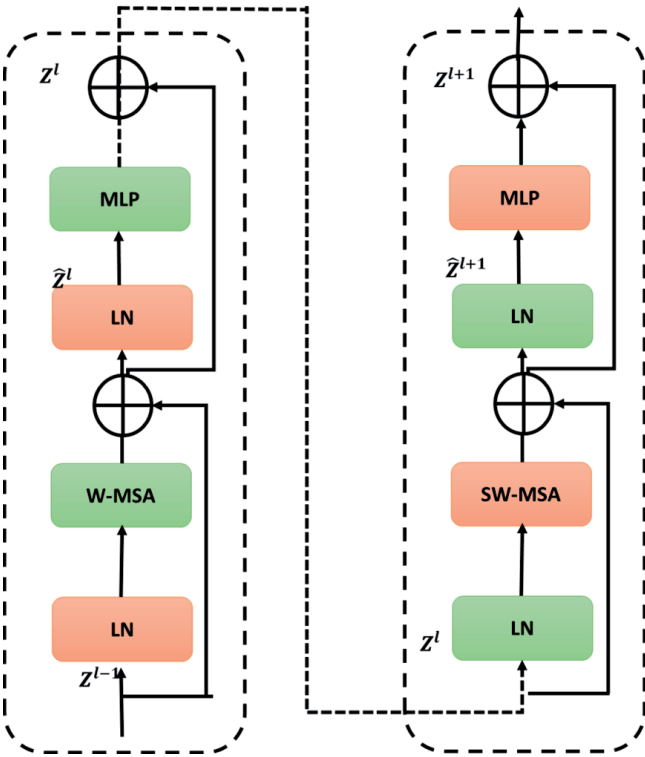


Fig. 3. Swin Transformer (ST) Block

Results and Discussion

Image segmentation is widely utilized in brain MRI analysis for a variety of purposes, including measurement and visualization of brain anatomical features, a study of brain changes, delineation of diseased areas, surgical planning, and image-guided treatments. In this article, we compared several of the available approaches, including Fuzzy clustering Algorithm (FCA), Fully convolutional network (FCN), and U-Net-based segmentation (UBS). We proposed the method Chaotic Atom Search optimized Swin transformer architecture. The behavior of the suggested strategy is verified using criteria like

1. Accuracy
2. Precision
3. Recall and
4. F1-Score

This assessment will take into account four factors: t_p stands for true positive, t_n for true negative, f_p for false positive, and f_n for false Negative.

Accuracy is a measure of how many samples are properly categorized. It determines the degree of similarity between the final results and the input data. Table shows the accuracy obtained for various models. The graph shown in Figure 4 demonstrates how the new technique is more accurate than the old one.

$$(4) \quad \text{Accuracy} = \frac{t_p + t_n}{t_p + t_n + f_p + f_n}$$

- t_p Represents a symbol of normalcy, and that's precisely what this picture is.
- t_n Represents that the image should be stegged, and in fact, it is stegged.
- f_p Represents the picture is not stegged although it is anticipated to be.
- f_n Represents that the picture is stegged even if it seems normal.

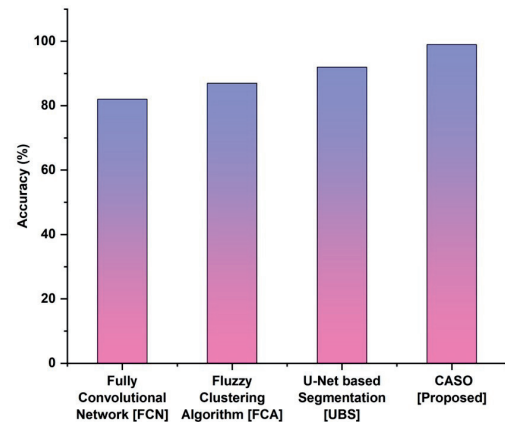


Fig. 4. Accuracy comparisons between the suggested and current approaches

The precision of the recommended Procedure by comparing the number of actual successes with the number of expected successes. The performance of the suggested technique is evaluated by distinguishing between true positives and false positives. The accuracy of both the current and suggested methods is compared in Figure 5. Compared to older approaches, the new one is more precise, as seen by the graph.

$$(5) \quad \text{Precision} = \frac{t_p}{t_p + f_p}$$

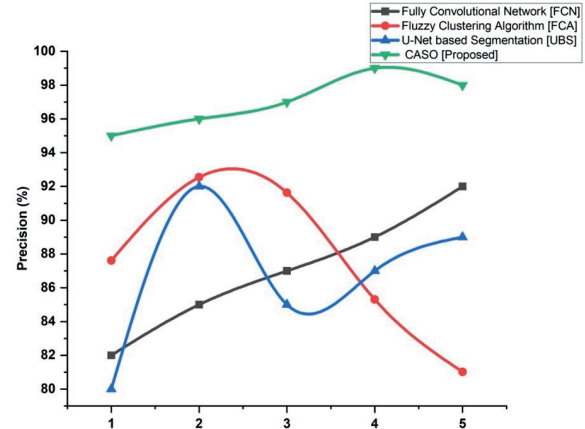


Fig. 5. Comparison of precision of the existing and proposed methodologies

The recall is the likelihood of a positive test on the assumption that it is positive. This is known as the actual positive rate. It reveals that the recall of the proposed methodology is superior than the recall of the earlier approaches. The sensitivity of the proposed technique to different parameters is compared to established approaches in Figure 6.

$$(6) \quad \text{Recall} = \frac{t_p}{t_p + f_n}$$

The F1-Score is often used while assessing information. It is possible to alter the F1-score so that accuracy is prioritized above recall, or vice versa. The recommended technique has a higher level of F1-score when measured against the currently used methods. In Figure 7, the f1-score of

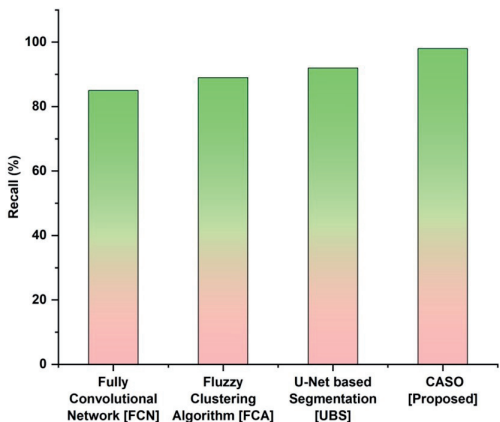


Fig. 6. The comparison of recall the proposed technique is compared to that of the traditional methods.

$$(7) \quad F1 - Score = \frac{2 \times precision \times recall}{precision + recall}$$

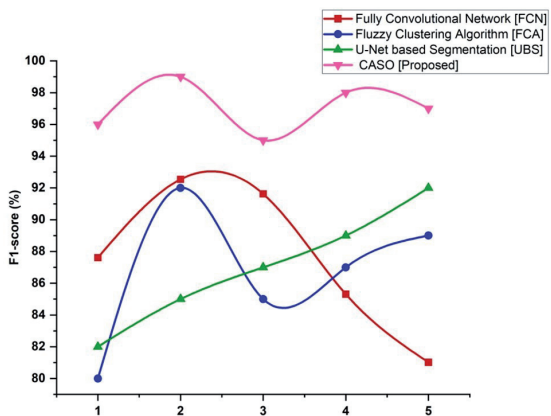


Fig. 7. Comparison of F1-score with Traditional and suggested techniques

Conclusion

This paper suggested Chaotic Atom search optimized Swin transformer Architecture for efficient Corpus callosum segmentation in Brain MRI images. Standardized data set such as OASIS is utilized to conduct an initial review during the research assessment. Extensive simulations have been run to assess the performance of the proposed network. Excellent outcomes are obtained with the proposed CASO for efficient CC segmentation in Brain MRI images. The recommended classification and extraction procedures perform better than the other extraction and classification techniques when compared to the outcomes of the other approaches. In the future, it may be possible to extract the CC using segmentation techniques like superpixels and local binary patterns. The suggested approach can also be used to assess brain scans taken from volunteers who have autism at the medical level.

Authors:

REFERENCES

- [1] Shai Berman, Shir Filo, and Aviv A Mezer. Modeling conduction delays in the corpus callosum using mri-measured g-ratio. *Neuroimage*, 195:128–139, 2019.
- [2] Ángela Bernabéu-Sanz, Sandra Morales, Valery Naranjo, and Ángel P Sempere. Contribution of gray matter atrophy and white matter damage to cognitive impairment in mildly disabled relapsing-remitting multiple sclerosis patients. *Diagnósticos*, 11(3):578, 2021.
- [3] J Blaauw and LC Meiners. The splenium of the corpus callosum: embryology, anatomy, function and imaging with pathophysiological hypothesis. *Neuroradiology*, 62:563–585, 2020.
- [4] J Blaauw and LC Meiners. The splenium of the corpus callosum: embryology, anatomy, function and imaging with pathophysiological hypothesis. *Neuroradiology*, 62:563–585, 2020.
- [5] J Blaauw and LC Meiners. The splenium of the corpus callosum: embryology, anatomy, function and imaging with pathophysiological hypothesis. *Neuroradiology*, 62:563–585, 2020.
- [6] Thais Caldeira, Paulo Rogério Julio, Simone Appenzeller, and Letícia Rittner. incsight: A software for exploration and visualization of dt-mri data of the corpus callosum. *Computers & Graphics*, 99:259–271, 2021.
- [7] Aaron Carass, Jennifer L Cuzzocreo, Shuo Han, Carlos R Hernandez-Castillo, Paul E Rasser, Melanie Ganz, Vincent Beliveau, Jose Dolz, Ismail Ben Ayed, Christian Desrosiers, et al. Comparing fully automated state-of-the-art cerebellum parcellation from magnetic resonance images. *Neuroimage*, 183:150–172, 2018.
- [8] Anjali Chandra, Shrish Verma, Ajay Singh Raghuvanshi, Narendra D Londhe, Narendra Kuber Bodhey, and Kumar Subham. Corpus callosum segmentation from brain mri and its possible application in detection of diseases. In *2019 IEEE International Conference on Electrical, Computer and Communication Technologies (ICECCT)*, pages 1–4. IEEE, 2019.
- [9] GS Cover, William Garcia Herrera, Mariana P Bento, Simone Appenzeller, and Letícia Rittner. Computational methods for corpus callosum segmentation on mri: A systematic literature review. *Computer methods and programs in biomedicine*, 154:25–35, 2018.
- [10] GS Cover, William Garcia Herrera, Mariana P Bento, Simone Appenzeller, and Letícia Rittner. Computational methods for corpus callosum segmentation on mri: A systematic literature review. *Computer methods and programs in biomedicine*, 154:25–35, 2018.
- [11] Chitraidevi Dhakhinamoorthy, Sathish Kumar Mani, Sandeep Kumar Mathivanan, Senthilkumar Mohan, Prabhu Jayagopal, Saurav Mallik, and Hong Qin. Hybrid whale and gray wolf deep learning optimization algorithm for prediction of alzheimer's disease. *Mathematics*, 11(5):1136, 2023.
- [12] Douglas N Greve, Benjamin Billot, Devani Cordero, Andrew Hoopes, Malte Hoffmann, Adrian V Dalca, Bruce Fischl, Juan Eugenio Iglesias, and Jean C Augustinack. A deep learning toolbox for automatic segmentation of subcortical limbic structures from mri images. *Neuroimage*, 244:118610, 2021.
- [13] Fidel Hernandez, Chiara Giordano, Maged Goubran, Sherven Parivash, Gerald Grant, Michael Zeineh, and David Camarillo. Lateral impacts correlate with falx cerebri displacement and corpus callosum trauma in sports-related concussions. *Biomechanics and modeling in mechanobiology*, 18:631–649, 2019.
- [14] Amanda K Huber, David A Giles, Benjamin M Segal, and David N Irani. An emerging role for eotaxins in neurodegenerative disease. *Clinical Immunology*, 189:29–33, 2018.
- [15] Paulo Rogério Julio, Thais Caldeira, Gustavo Retuci Pinheiro, Carla Helena Capello, Renan Bazuco Fritolli, Roberto Marini, Fernando Cendes, Paula Teixeira Fernandes, Lilian TL Costalat, Letícia Rittner, et al. Microstructural changes in the corpus callosum in systemic lupus erythematosus. *Cells*, 12(3):355, 2023.
- [16] Mónica López-Vicente, Sander Lamballais, Suzanne Louwen, Manon Hillegers, Henning Tiemeier, Ryan L Muetzel, and Tonya White. White matter microstructure correlates of age, sex, handedness and motor ability in a population-based sample of 3031 school-age children. *Neuroimage*, 227:117643, 2021.
- [17] Siuly Siuly and Yanchun Zhang. Medical big data: neurological diseases diagnosis through medical data analysis. *Data Science and Engineering*, 1:54–64, 2016.
- [18] Stefanus E Sugijono, Rahmad Mulyadi, Salsabila Firdausia, Joedo Prihartono, and Riwanti Estiasari. Corpus callosum index correlates with brain volumetry and disability in multiple sclerosis patients. *Neurosciences Journal*, 25(3):193–199, 2020.
- [19] Lara M Wierenga, Marieke GN Bos, Elisabeth Schreuders, Ferdi vd Kamp, Jiska S Peper, Christian K Tamnes, and Eveline A Crone. Unraveling age, puberty and testosterone effects on subcortical brain development across adolescence. *Psychoneuroendocrinology*, 91:105–114, 2018.